Stacking order-dependent sign-change of microwave phase due to eddy currents in nanometer-scale NiFe/Cu heterostructures

O. Gladii, R L Seeger, L. Frangou, G. Forestier, U. Ebels, S. Auffret, Vincent Baltz

Stacking order-dependent sign-change of microwave phase due to eddy currents in nanometer-scale NiFe/Cu heterostructures

O. Gladii,[*] R. L. Seeger,[*] L. Frangou,[*] G. Forestier, U. Ebels, S. Auffret, and V. Baltz[**]

SPINTEC, Univ. Grenoble Alpes / CNRS / INAC-CEA / GINP, F-38000 Grenoble, France

[*] *equal contribution*

[**] *vincent.baltz@cea.fr*

Abstract

In the field of spintronics, ferromagnetic/non-magnetic metallic multilayers are core building blocks for emerging technologies. Resonance experiments using stripline transducers are commonly used to characterize and engineer these stacks for applications. Up to now in these experiments, the influence of eddy currents on the dynamics of ferromagnetic magnetization below the skin-depth limit was most often neglected. Here, using a coplanar stripline transducer, we experimentally investigated the broadband ferromagnetic resonance response of NiFe/Cu bilayers a few nanometers thick in the sub-skin-depth regime. Asymmetry in the absorption spectrum gradually built up as the excitation frequency and Cu-layer thickness increased. Most significantly, the sign of the asymmetry depended on the stacking order. All experimental data were consistent with a quantitative analysis considering eddy currents generated indirectly in the Cu layers by the time varying magnetic field due to oscillation of the NiFe layer's magnetization, and the subsequent phaseshift of the feedback magnetic field generated by the eddy currents. These results extend our understanding of the impact of eddy currents below the microwave magnetic skin-depth and explain the lineshape asymmetry and phase lags reported in stripline experiments.

Keywords: ferromagnetic resonance, eddy currents, sub-skin-depth, lineshape, phaseshift

Resonance experiments are a powerful means to study physical systems and facilitate advances in material characterization and engineering. In the field of spintronics, ferromagnetic/non-magnetic (F/NM) metallic multilayers are core building blocks for emerging technologies.[1] In these multilayers, the physical properties of the F (effective magnetization, anisotropy, damping), the NM metal (spin penetration length, relaxation mechanisms, eddy currents) and the interface (spin filtering, roughness) can all be recorded by measuring ferromagnetic resonance (FMR) spectra and determining their position, linewidth, and lineshape.[2]

Lineshape asymmetries are relatively common in ferromagnetic resonance experiments performed with stripline setups (coplanar and microstrip). The part of the stripline inductively coupled to the sample is equivalent to a device circuit defining a complex microwave impedance.[3–5] The resulting phase of the microwave excitation leads to an absorption-dispersion admixture and produces asymmetric lineshapes. Although a parameter accounting for such asymmetry must be considered if the spectral position and linewidth are to be accurately extracted from data fitting, it is usually not commented on. The reason for this omission is, first, because asymmetry, linewidth and position are not related; and, second, because for most geometries used in FMR experiments, the absorption component prevails[4] and this type of *experiment-related asymmetry* is therefore small.

In addition to inductive coupling, other effects such as eddy currents may produce unusual lineshapes. This type of effect has been thoroughly studied for film thicknesses above the skin-depth limit.[6] In contrast, below this limit, the effects of eddy currents were most often neglected, except for series of comprehensive studies focused on microwave screening/shielding,[4,5,7,8] e.g. leading to layer-transducer ordering-dependent standing spin wave modes in sufficiently thick layers[4,7] and to depth-dependent dephasing.[8] Some recent experimental studies on F-NiFe(10nm)/NM-(Au,Cu) bilayers[9,10] revealed how the Oersted field

- due to eddy currents in the NM layer - also affects the dynamics of F magnetization, and more specifically, how it creates additional phase lags resulting in distortion of the resonance lineshape. The experiments were performed in a cavity setup and corroborated the results of analytical calculations. The scenario considered in Refs. [9,10] involved eddy currents in the NM conductor, generated directly by an excitation radiofrequency magnetic field ($\mathbf{h}_{rf}$) applied out-of-plane. The phaseshift between $\mathbf{h}_{rf}$ and the eddy current-induced field contributed to dephasing of the NiFe magnetization dynamics. This dephasing translated into an absorption-dispersion admixture of the signal and produced an asymmetric resonance line. In this scenario, experiments conducted with stripline setups, with $\mathbf{h}_{rf}$ in the sample plane, should not generate eddy currents in the conductive layers. However, it has been suggested that non-uniformity of the microwave field or sample tilting would lead to an out-of-plane component of $\mathbf{h}_{rf}$, [9] thus creating the conditions for *eddy current-related asymmetry*, as in the 'direct' scenario described above. According to this hypothesis, the sign of the lineshape asymmetry should be independent of the stacking order for the layers. The data show that this assumption fails to completely describe experimental results.

In this article, the incompletely understood impact of eddy currents is investigated and we unravel the contributions to lineshape asymmetry in stripline experiments. We chose to study the broadband FMR response in NiFe/Cu bilayers a few nanometers thick. Our results revealed a frequency- and Cu-thickness-dependent asymmetry, the sign of which most significantly depends on the Cu to NiFe layer stacking order.

The full stacks used in this study were (from substrate to surface): $Cu(t_{Cu})/NiFe(t_{NiFe})/Al(2)Ox$ and $NiFe(t_{NiFe})/Cu(t_{Cu})/Al(2)Ox$ multilayers. All thicknesses are given in nanometers. t_{Cu} is the thicknesses of the Cu layer and was varied between 1 and 14 nm; t_{NiFe} is the thicknesses of the NiFe layer: t_{NiFe} = 4, 8, or 12 nm. Stacks were deposited at room

temperature by dc-magnetron sputtering on thermally-oxidized silicon substrates [$Si/SiO_2(500)$] at a working pressure of argon of 2.3 x 10^{-3} mbar. The NiFe layer was deposited from a $Ni_{81}Fe_{19}$ (at. %) permalloy target. A 2-nm-thick Al cap was deposited to form a protective Al(2)Ox film after oxidation in air. This insulating film also prevented direct electrical contact between the samples and the waveguide (Fig. 1(a,b)). Unless specified otherwise, the sample dimensions were: l = 4 mm, w = 3 mm. The microwave transducer consisted of a double-ground plane broadband coplanar waveguide. The width of the central conductor strip was 375 μm and the gap between the central line and the ground planes on each side was 140 μm. A Schottky diode converted the electromagnetic field into a voltage and was used for detection. Modulation coils and lock-in detection were used to enhance the signal-to-noise ratio. FMR experiments and the corresponding differential absorption spectra, $d\chi''/dH$ *vs.* H (Fig. 1(c-h)), were recorded at room temperature at frequencies ranging between 4 and 20 GHz.

First, we discuss the spectrum asymmetry which gradually built up as the t_{Cu} increased (Fig. 1(c-h)). This behavior revealed a non-negligible impact of eddy currents circulating in the Cu layers, mostly along the edges. Most importantly, the sign of the asymmetry depended on the ordering of the Cu and NiFe layers, i.e., whether the Cu layer was the buffer or capping layer. A scenario involving eddy currents generated directly by $\mathbf{h}_{rf}$, like in Ref. [9] cannot readily explain the sign-change observed here for the capping and buffer layer cases. Rather, we considered that the oscillation of the NiFe magnetization generated a time varying out-of-plane magnetic field ($\mathbf{h}_M$) and a related magnetic flux variation which created eddy currents in the plane of the adjacent Cu layers. In return, the eddy currents generated a feedback rf magnetic field ($\mathbf{h}_{FB}$) that contributes to the dephasing of the NiFe magnetization dynamics (Fig. 1(a,b)). In this scenario, $\mathbf{h}_{FB}$ for the buffer and capping Cu layers would naturally be in antiphase to one

another. To extract the asymmetry and quantify the findings, the differential resonance spectra were fitted with the following equation:[9]

$$\chi'' \propto \frac{1+\beta(H-H_{res})/(\sqrt{3}\Delta H_{pp})}{(H-H_{res})^2+(\sqrt{3}\Delta H_{pp}/2)^2} \quad (1),$$

where H_{res} is the resonance field, ΔH_{pp} is the peak-to-peak linewidth, and β is the asymmetry parameter accounting for absorption-dispersion admixtures due to the relative phase shift (φ) between $\mathbf{h}_{FB}$, and $\mathbf{h}_{M}$.

Figure 2(a) shows β plotted as a function of t_{Cu} for series of Cu(t_{Cu})/NiFe(t_{NiFe}=4;8;12)/Al(2)Ox ('buffer') and NiFe(t_{NiFe}=4;8;12)/Cu(t_{Cu})/Al(2)Ox (nm) ('capping') multilayers. The gradual increase in $|\beta|$ with t_{Cu} agrees with the fact that eddy currents relate to the conductance of the Cu layers, which increases with t_{Cu}. The above deductions can, indeed, be correlated by applying simple models. Adapting the formulation suggested in Ref. [9] to our case, we obtain:

$$\beta = \frac{h_{FB}\sin(\varphi)}{h_M + h_{FB}\cos(\varphi)} + \beta_0 \quad (2).$$

where β_0 is the residual *experiment-related* phaseshift. Here, we considered the asymmetry created by out-of-plane fields (β_y), as justified below, and consequently we neglected the contribution of h_{rf}. The field h_{FB} relates to the rate of change of magnetic flux through the area delimited by the eddy current loop. It can be expressed as $h_{FB} = \frac{\mu_0 lw\pi f t_{Cu}}{2(l+w)\rho} h_M$,[9] where ρ is the Cu layer's resistivity, which can be taken as inversely proportional to t_{Cu} in the thickness range investigated (1-14 nm): $\rho = \eta / t_{Cu}$, where η is the proportionality factor, in line with the Fuchs-Sondheimer model.[11,12] We neglected the contribution of the skin effect to the phaseshift, which is proportional to t_{Cu}/δ_{Cu},[13] because t_{Cu}=1-14 nm, and the skin-depth δ_{Cu}~1000-500 nm for f=4-20 GHz. In the ideal situation of negligible inductive contribution $\varphi = -\pi/2$, and $\varphi = \pi/2$ for

the ‘capping’ and ‘buffer’ layer cases, respectively. Developing the different terms in Eq. (2) produced a quadratic dependence of β on t_{Cu}, and a linear dependence on *f* and on the sample-area-to-perimeter-ratio:

$$\beta = \pm A f t_{Cu}^2 + \beta_0, \text{ with } A = \frac{\mu_0 l w \pi}{2(l+w)\eta} \quad (3).$$

The straight blue line in Fig. 2(a) was fitted with Eq. (3), and returned A=1x10^{-3} GHz^{-1}.nm^{-2} and β_0 =-0.3. The value for A gives a reasonable resistivity for Cu: $\rho[\mu\Omega.cm] = 350 / t_{Cu}[nm]$. From Fig. 2(a), it can be seen that the simplified model captures the physics of the phenomenon observed. However, deviations between predictions and experimental data can be observed for the ‘buffer’ layer case. First, both the resistivity and the eddy current path in the capping and buffer Cu layer are likely to differ due to the inversion of the growth order. The prefactor A in Eq. (3) is therefore likely to depend on the ‘capping’ and ‘buffer’ nature of the Cu layer. Second, the t_{Cu}-dependence of the layer’s resistivity may differ from the inverse proportionality law we considered. Third, and most importantly for thick Cu layers and high frequencies, inductive contributions are very likely to affect the ideal t_{Cu}^2-dependence of β in a non-trivial manner. Considering an inductive term, the phase shift becomes: $\varphi = \pm\pi/2 + \theta(f, t_{Cu}, l, w, \zeta)$, where $\theta(f, t_{Cu}, l, w, \zeta)$ shows a non-linear dependence on several parameters: f, t_{Cu}, l, w, and ζ, the unknown width of the eddy current loops circulating along the perimeter of the 4x3 mm^2 Cu layer. This width will be discussed further below. Rewriting Eq. (2) then gives:

$$\beta = \frac{A f t_{Cu}^2 \sin(\pm\pi/2 + \theta(f, t_{Cu}, l, w, \zeta))}{1 + A f t_{Cu}^2 \cos(\pm\pi/2 + \theta(f, t_{Cu}, l, w, \zeta)} + \beta_0 \quad (4).$$

The non-trivial influence of the inductive contributions can clearly be seen for *f*-dependent measurements. Figure 2(b) shows β vs. *f*, for series of Cu(t_{Cu}=1;8;14)/NiFe(8)/Al(2)Ox ‘buffer’ and NiFe(8)/Cu(t_{Cu}=1;8;14)/Al(2)Ox (nm) ‘capping’ multilayers. Data for t_{Cu}=1 nm, in the absence of eddy current, correspond to β_0 and

superimpose for the 'buffer' and 'capping' cases. The *f*-dependence of β_0 is weak, ruling out any *f*-dependent impedance contribution of the NiFe layer to the phaseshift. The straight lines in Fig. 2(b) were produced by calculations using Eq. (3). The same set of parameters as that returned from Fig. 2(a) was used. This same set of parameters satisfactorily and concurrently described the t_{Cu}^2- and *f*-dependences of β for the 'capping' case (Fig. 2(b)), confirming that the simplified model reflects the physics behind the phenomenon observed. The overall linear increase of $|\beta|$ with *f*, driven by the fact that eddy currents increase when the rate of change of flux rises, may be altered by complex inductive contributions, which are known to increase for higher frequencies and thicker films. In agreement with this information, we observe in Fig. 2(b) that data depart from a linear dependence above 10 GHz for the 14-nm-thick capping layer, a result that contrasts with those obtained for the 8-nm-thick one, which follows a linear dependence throughout. Similarly, data for the 8-nm-thick buffer layer obey a linear dependence throughout, unlike the 14-nm-thick buffer layer. The latter case typically illustrates how non-trivial inductive contributions to β can drastically distort and bend the initially linear *f*-dependence. To rule out any contribution of the [Si/SiO_2(500)] substrate on the stacking order-dependent sign-change of β, we compared a Cu(14)/NiFe(4)/Al(2)Ox to a NiFe(4)/Cu(14)/Al(2)Ox (nm) stack deposited on glass substrates (not shown). The same trend of a positive vs. negative value of β for the 'capping' vs. 'buffer' case was obtained.

We will now consider finite-size effects. Once again using Fig. 2(a), we will briefly comment on the square crossed symbol corresponding to data recorded after patterning only the Cu(14)/Al(2)Ox capping layers in a Si/SiO_2/NiFe(8)/Cu(14)/Al(2)Ox (nm) stack (inset of Fig. 2(a)). A 4 x 3 mm^2 array of square dots with lateral size of 100 μm was fabricated. Following patterning, two effects compete with one another. First, the number of eddy current loops increases, and simultaneously, the path of each loop along the sample's edges is constrained.

The fact that patterning significantly reduced β to a value close to β_0 (Fig. 2(a)) shows that eddy currents cannot develop in the dots. This result indicates that the dot size (100 µm) was roughly smaller than twice the width of the eddy current loop. We further assessed the dependence of β on the sample's area-to-perimeter-ratio, $lw/[2(l+w)]$ (Fig. 3(a)). A linear dependence was found, as anticipated from Eq. (3). Data fitting with Eq. (3) returned β_0 =0.3, and a slope of 1.95 mm^{-1}, corresponding to $\rho[\mu\Omega.cm] = 395/t_{Cu}[nm]$. This value is in reasonable agreement with that obtained from the t_{Cu}^2 - and *f*-dependence presented above (Fig. 2). The discrepancy for the β_0 value is probably related to the non-trivial inductive effects discussed above. Figures 3(b,c) present control data showing that the sample vs. stripline dimensions remained within a range where the linewidth and position were unaffected by geometrical effects. To conclude with size effects, our results show that rotating the sample in the plane of the stripline (l // h_{rf} vs. w // h_{rf}) had no impact on the data (Fig. 3(a)), demonstrating that both the length and the width of the current path contribute to h_{FB}, and that the *y* contribution of β (see Fig. 1) matters in this context, unlike with other geometries, where the *x* contribution seemed to dominate.[9]

Before concluding the paper, we will briefly comment on the position (H_{res}) and the width (ΔH_{pp}) of the spectra (Eq. (1)), although they are not the focus of this article. The total Gilbert damping, α, was calculated from the slope of *f*-dependent measurements (ΔH_{pp} vs. f), from $\Delta H_{pp} = \Delta H_{pp0} + 4\pi\alpha f/(\sqrt{3}|\gamma|)$,[14] where ΔH_{pp0} is the inhomogeneous broadening[15] due to spatial variations in the magnetic properties (values of a few Oe were measured in our experiments) and γ is the gyromagnetic ratio (derived from the fit of the curve representing H_{res} vs. f). Plots representing H_{res} vs. t_{Cu} and α vs. t_{Cu} are shown in Figs. 4(a,b) and Figs. 4(c,d), respectively. As expected, the data showed no obvious link between spectrum asymmetry (Fig. 2), and spectrum position, H_{res} and width (see H_{res} and α, Fig. 4). For t_{NiFe} = 4

nm, a non-monotonous dependence of H_{res} was observed. This behavior supports non-monotonous dependence of the effective NiFe magnetization, M_{eff}, (Figs. 4(e,f)) which can be extracted from H_{res} vs. f using the Kittel formula:[16] $(2\pi f)^2 = |\gamma| H_{res}(H_{res} + 4\pi M_{eff})$. We recall that $M_{eff} = M_S - 2K_S/(4\pi M_S t_{NiFe})$, where M_S is the saturation magnetization. The values of M_S (Fig. 4(g,h)), measured independently by magnetometry, were monotonous and thus confirmed that the non-monotonous behavior of M_{eff} seems to primarily relate to the properties of the Cu/NiFe interface. A similar non-monotonous dependence of α was observed. Cu wets poorly on SiO_2 compared to NiFe on SiO_2 and Cu, and as a result may create rougher thin Cu films. Consequently, spatially inhomogeneous stray fields may lead to incoherent dephasing of the spin current[17,18] injected from the NiFe to the Cu, and thus to enhanced damping. Varying the capping layer thickness thus has virtually no influence on damping, in agreement with the observations.

In conclusion, the main contribution of this paper is that it represents systematic experimental evidence of a stacking-order-dependent sign-change of the microwave phase in nanometer-scale NiFe/Cu bilayers. The effect could be ascribed to eddy currents generated indirectly in the Cu layer in the sub-skin-depth regime by the time varying magnetic field due to oscillation of the NiFe layer's magnetization. Three distinct sets of experimental data were consistent with a simple quantitative analysis encompassing the main features of the phenomenon. These results contribute to our understanding of the impact of eddy currents below the microwave magnetic skin-depth and explain the contributions to lineshape asymmetry and phase lags reported in stripline experiments commonly used to characterize and engineer materials for spintronic applications.

Acknowledgments

We acknowledge financial support from the French national research agency (ANR) [Grant Number ANR-15-CE24-0015-01] and KAUST [Grant Number OSR-2015-CRG4-2626]. We also thank M. Gallagher-Gambarelli for critical reading of the manuscript.

References

[1] R.L. Stamps et al, J. Phys. D. Appl. Phys. **47**, 1 (2014).

[2] W.E. Bailey, in *Introd. to Magn. Random-Access Mem.* (John Wiley & Sons, Ltd, 2016).

[3] W. Heinrich, IEEE Trans. Microw. Theory Tech. **41**, 45 (1993).

[4] I.S. Maksymov and M. Kostylev, Phys. E **69**, 253 (2015).

[5] M. Bailleul, Appl. Phys. Lett. **103**, 192405 (2013).

[6] F.J. Dyson, Phys. Rev. **98**, 349 (1955).

[7] K.J. Kennewell, M. Kostylev, N. Ross, R. Magaraggia, R.L. Stamps, M. Ali, A.A. Stashkevich, D. Greig, and B.J. Hickey, J. Appl. Phys. **108**, 73917 (2010).

[8] W.E. Bailey, C. Cheng, R. Knut, O. Karis, S. Auffret, S. Zohar, D. Keavney, P. Warnicke, J.-S. Lee, and D.A. Arena, Nat. Commun. **4**, 2025 (2013).

[9] V. Flovik, F. Macia, A.D. Kent, and E. Wahlstrom, J. Appl. Phys. **117**, 143902 (2015).

[10] V. Flovik, B.H. Pettersen, and E. Wahlström, J. Appl. Phys. **119**, 163903 (2016).

[11] K. Fuchs, Math. Proc. Cambridge Philos. Soc. **34**, 100 (1938).

[12] E.H. Sondheimer, Adv. Phys. **1**, 1 (1952).

[13] J.D. Jackson, *Classical Electrodynamics* (1962).

[14] C.E. Patton, J. Appl. Phys. **39**, 3060 (1968).

[15] E. Schlömann, Phys. Rev. **182**, 632 (1969).

[16] C. Kittel, Phys. Rev. **73**, 155 (1948).

[17] S.P. Dash, S. Sharma, J.C. Le Breton, J. Peiro, H. Jaffrès, J.-M. George, A. Lemaitre, and R. Jansen, Phys. Rev. B **84**, 54410 (2011).

[18] Y. Tserkovnyak, A. Brataas, G.E.W. Bauer, and B.I. Halperin, Rev. Mod. Phys. **77**, 1375 (2005).

Figure captions

Fig. 1. (color online) (a,b) Schematic representations of the coplanar waveguide (CPW) – FMR experiment. Samples were placed face-down on the waveguide. The in-plane dc bias field (**H**), the excitation magnetic field from the waveguide ($\mathbf{h_{rf}}$), the resulting out-of-plane field from the NiFe resonator ($\mathbf{h_M}$), and feedback field ($\mathbf{h_{FB}}$) from the eddy currents (I_{eddy}) induced by $\mathbf{h_M}$, are represented. (c-h) Representative differential absorption spectra ($d\chi''/dH$ *vs.* H) measured for $Si/SiO_2/NiFe(8)/Cu(t_{Cu})/Al(2)Ox$ and $Si/SiO_2/Cu(t_{Cu})/NiFe(8)/Al(2)Ox$ (nm) stacks. The straight lines were fitted to the data using a model derived from Ref. [9], which is described in the text. Data-fitting allowed the resonance field (H_{res}), the peak-to-peak line width (ΔH_{pp}), and the asymmetry parameter (β) to be determined.

Fig. 2. (color online) (a) Representative series of dependences of β on 'capping' and 'buffer' Cu-layer thickness (t_{Cu}) for $Si/SiO_2/Cu(t_{Cu})/NiFe(t_{NiFe}=4;8;12)/Al(2)Ox$ and $Si/SiO_2/NiFe(t_{NiFe}=4;8;12)/Cu(t_{Cu})/Al(2)Ox$ (nm) stacks. Data were recorded at 10 GHz. The square crossed symbol corresponds to data recorded after patterning (inset) the Cu(14)/Al(2)Ox bilayer in a $Si/SiO_2/NiFe(8)/Cu(14)/Al(2)Ox$ (nm) stack. The open square symbol corresponds to data for the same stack on which the whole etching process was performed, as these samples were protected by a resist they remained unpatterned. (b) Representative series of dependences of β on frequency (f) for $Si/SiO_2/Cu(t_{Cu}=1;8;14)/NiFe(8)/Al(2)Ox$ and $Si/SiO_2/NiFe(8)/Cu(t_{Cu}=1;8;14)/Al(2)Ox$ (nm) stacks. The straight lines in (a) and (b) were obtained using the model described in the text. The dash-dotted lines are visual guides.

Fig. 3. (color online) (a) Dependences of β on the sample's area (lw) to perimeter ($2((l+w))$) ratio for $Si/SiO_2/NiFe(8)/Cu(14)/Al(2)Ox$ (nm) stacks for two sample's orientations: $l // h_{rf}$ and

w // h$_{rf}$. Data were recorded at 10 GHz. The line was obtained using the model described in the text. (b,c) Corresponding dependences of H_{res} and ΔH_{pp}.

Fig. 4. (color online) Dependences of (a,b) H_{res}, (c,d) α, (e,f) M_{eff}, and (g,h) M_S on t_{Cu} for $Si/SiO_2/Cu(t_{Cu})/NiFe(t_{NiFe}=4;8;12)/Al(2)Ox$ and $Si/SiO_2/NiFe(t_{NiFe}=4;8;12)/Cu(t_{Cu})/Al(2)Ox$ (nm) stacks. The square crossed symbols correspond to the patterned sample. (a-b) correspond to data recorded at 10 GHz. (c-d) were deduced from *f*-dependences of ΔH_{pp}. (e,f) were deduced from *f*-dependences of H_{res}. (g,h) were measured independently by magnetometry, using a superconducting quantum interference device.

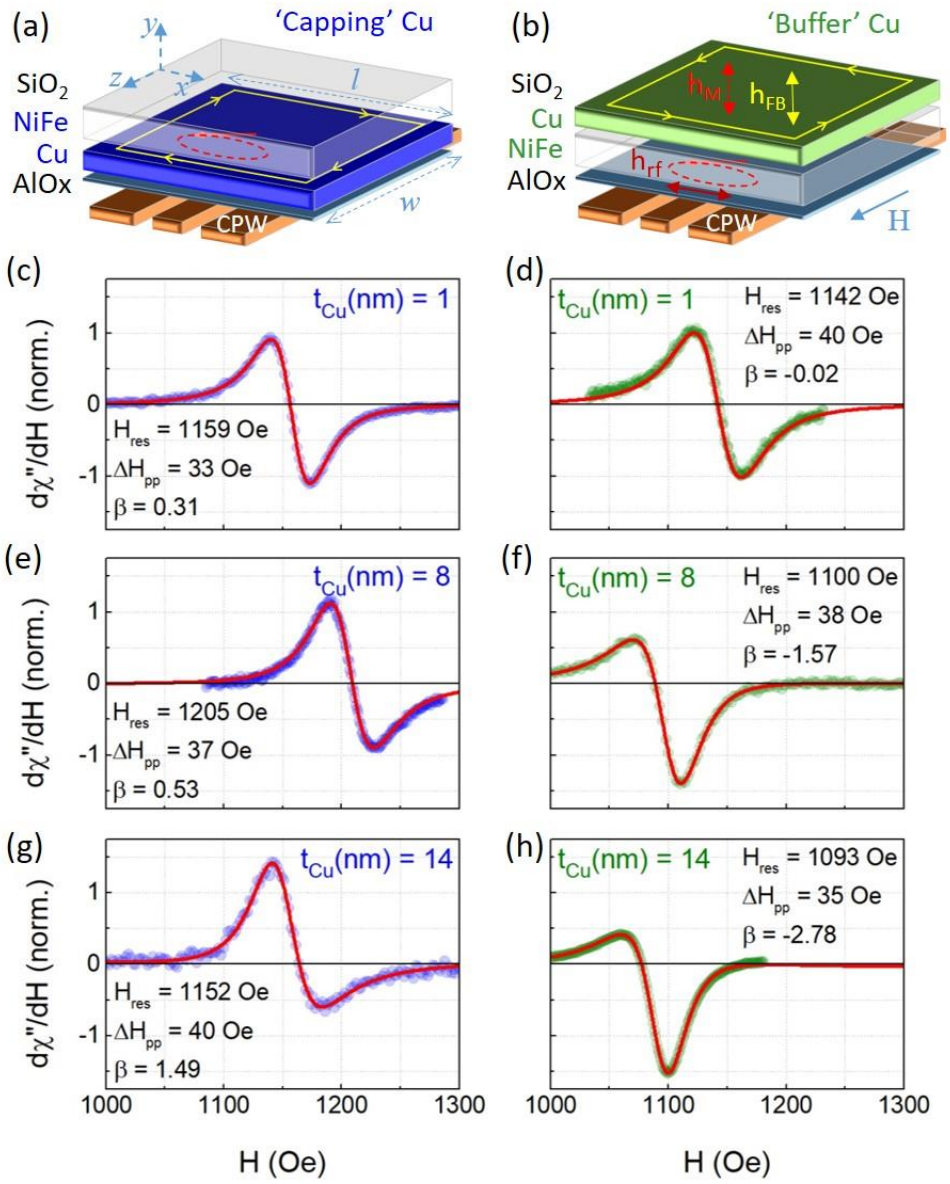
(a)
'Capping' Cu
SiO2
NiFe
Cu
AlOx
CPW
(b)
'Buffer' Cu
SiO2
Cu
NiFe
AlOx
CPW
H
(c)
tCu(nm) = 1
Hres = 1159 Oe
ΔHpp = 33 Oe
β = 0.31
(d)
tCu(nm) = 1
Hres = 1142 Oe
ΔHpp = 40 Oe
β = -0.02
(e)
tCu(nm) = 8
Hres = 1205 Oe
ΔHpp = 37 Oe
β = 0.53
(f)
tCu(nm) = 8
Hres = 1100 Oe
ΔHpp = 38 Oe
β = -1.57
(g)
tCu(nm) = 14
Hres = 1152 Oe
ΔHpp = 40 Oe
β = 1.49
(h)
tCu(nm) = 14
Hres = 1093 Oe
ΔHpp = 35 Oe
β = -2.78
dχ"/dH (norm.)
H (Oe)

Fig. 1

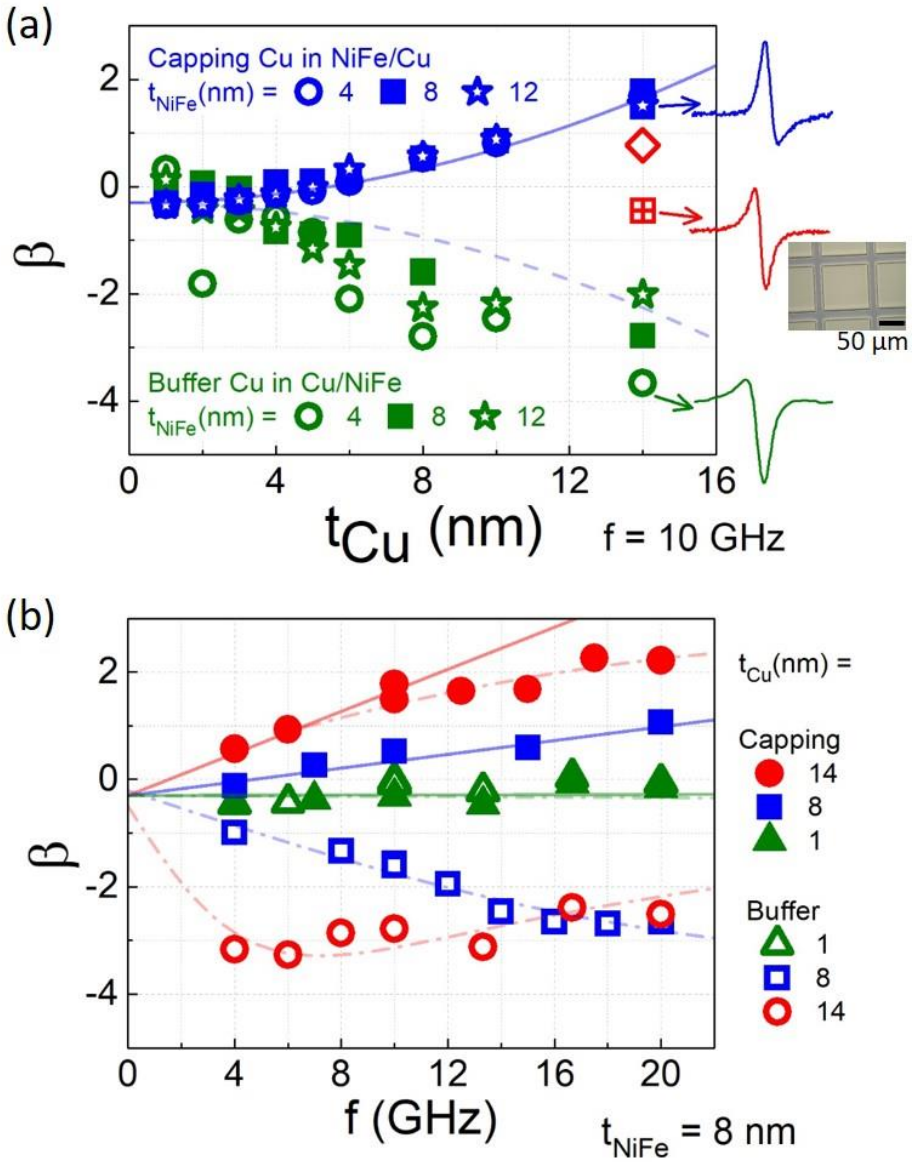
(a)
Capping Cu in NiFe/Cu
t_{NiFe}(nm) = 4 8 12
Buffer Cu in Cu/NiFe
t_{NiFe}(nm) = 4 8 12
β
t_{Cu} (nm)
f = 10 GHz
50 μm
(b)
t_{Cu}(nm) =
Capping
14
8
1
Buffer
1
8
14
β
f (GHz)
t_{NiFe} = 8 nm

Fig. 2

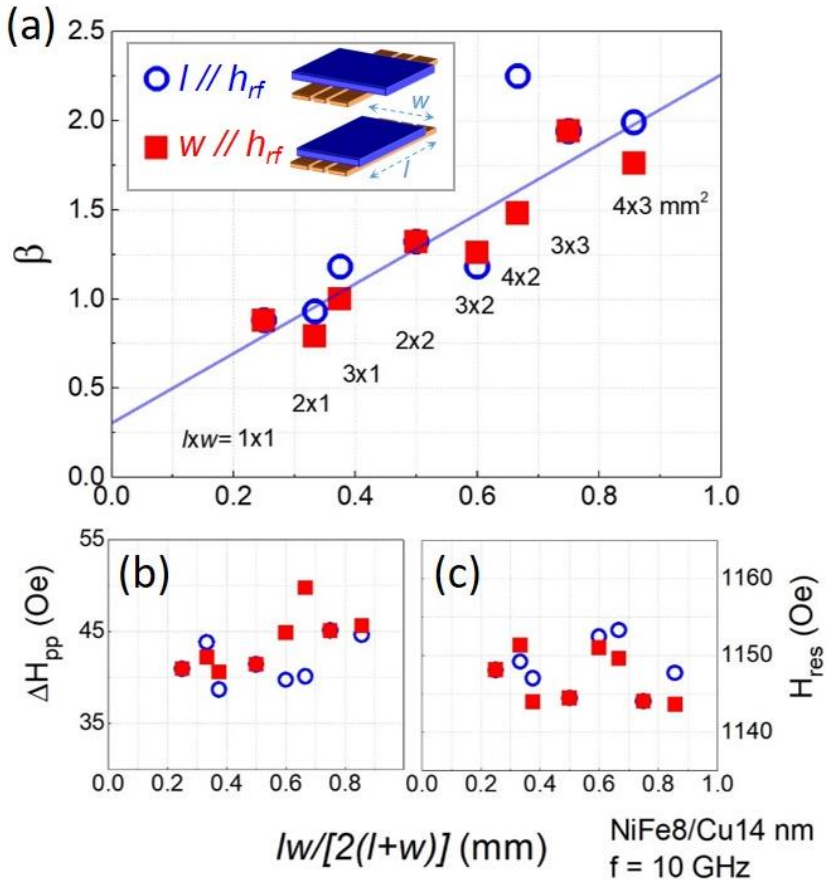
(a)
β
l // h_rf
w // h_rf
w
l
4x3 mm²
3x3
4x2
3x2
2x2
3x1
2x1
lxw= 1x1
(b)
ΔH_pp (Oe)
(c)
H_res (Oe)
lw/[2(l+w)] (mm)
NiFe8/Cu14 nm
f = 10 GHz

Fig. 3

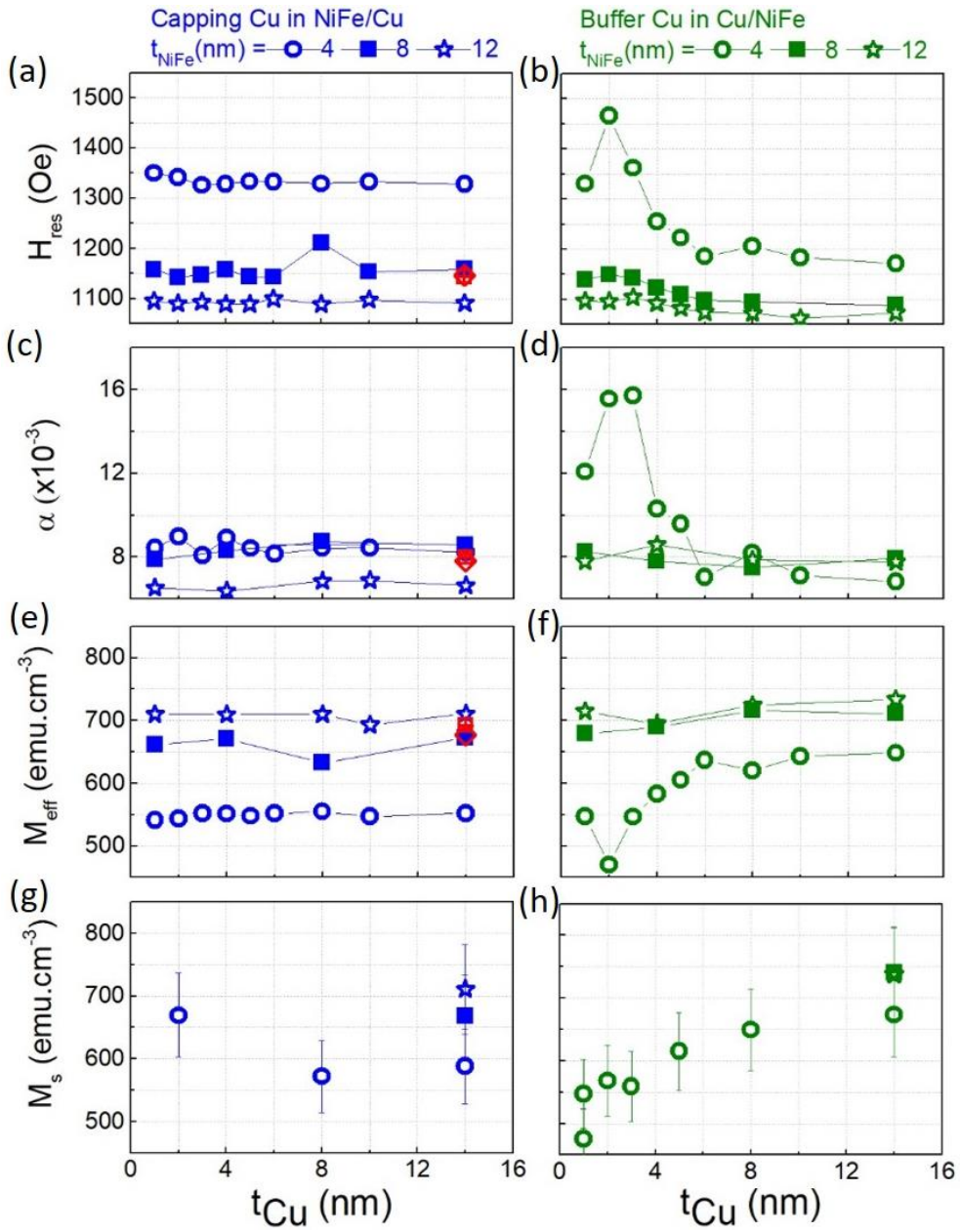
Capping Cu in NiFe/Cu
t_{NiFe}(nm) = 4 8 12
Buffer Cu in Cu/NiFe
t_{NiFe}(nm) = 4 8 12
(a)
(b)
(c)
(d)
(e)
(f)
(g)
(h)
H_{res} (Oe)
α (x10^{-3})
M_{eff} (emu.cm^{-3})
M_s (emu.cm^{-3})
t_{Cu} (nm)
t_{Cu} (nm)

Fig. 4